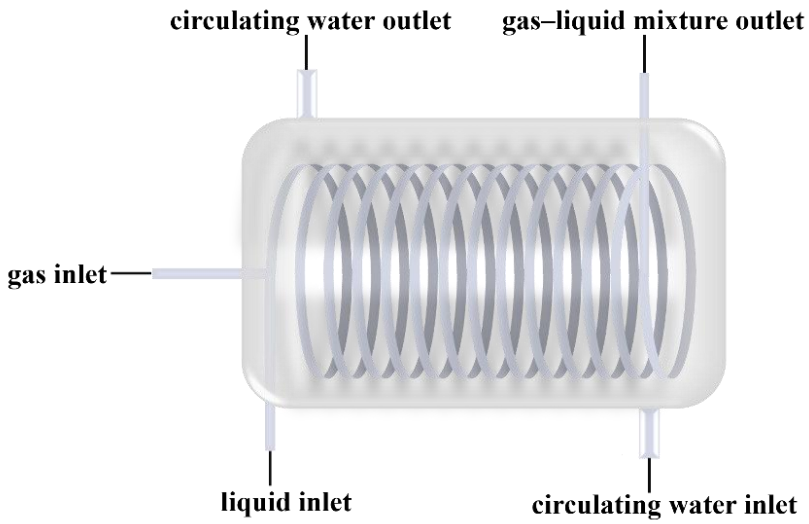

Figure S1. Structural diagram of the glass spiral coil

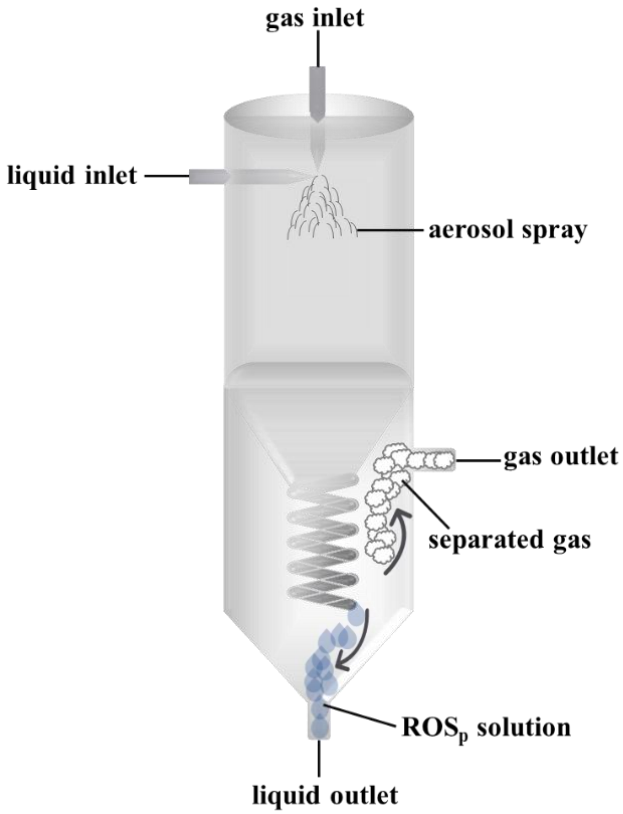

Figure S2. Structural diagram of the spray growth collection chamber

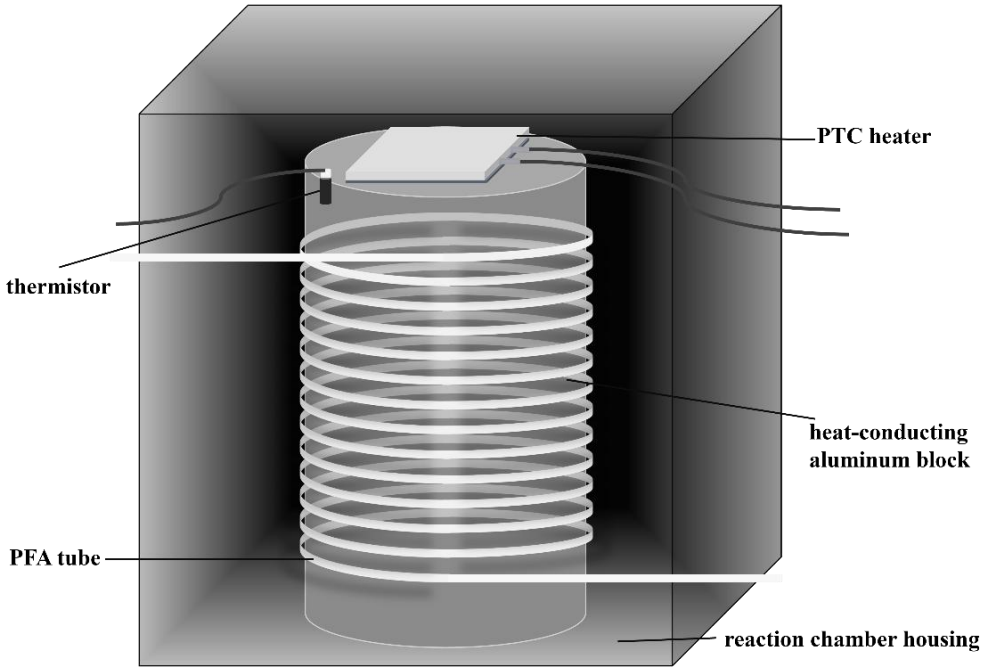

Figure S3. Structural diagram of the reaction chamber

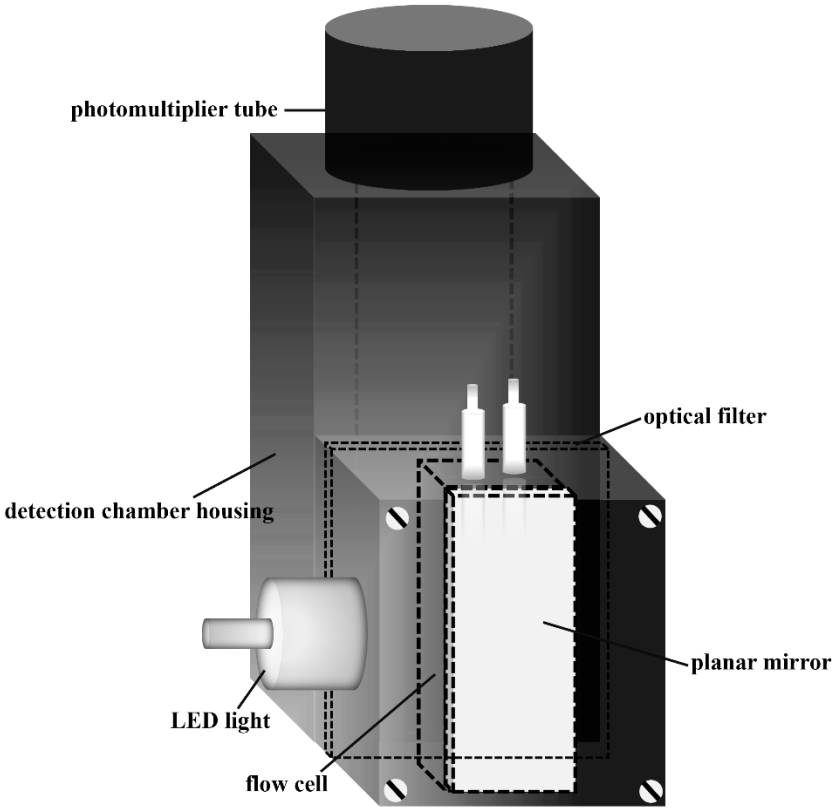

Figure S4. Structural diagram of the fluorescence detection chamber

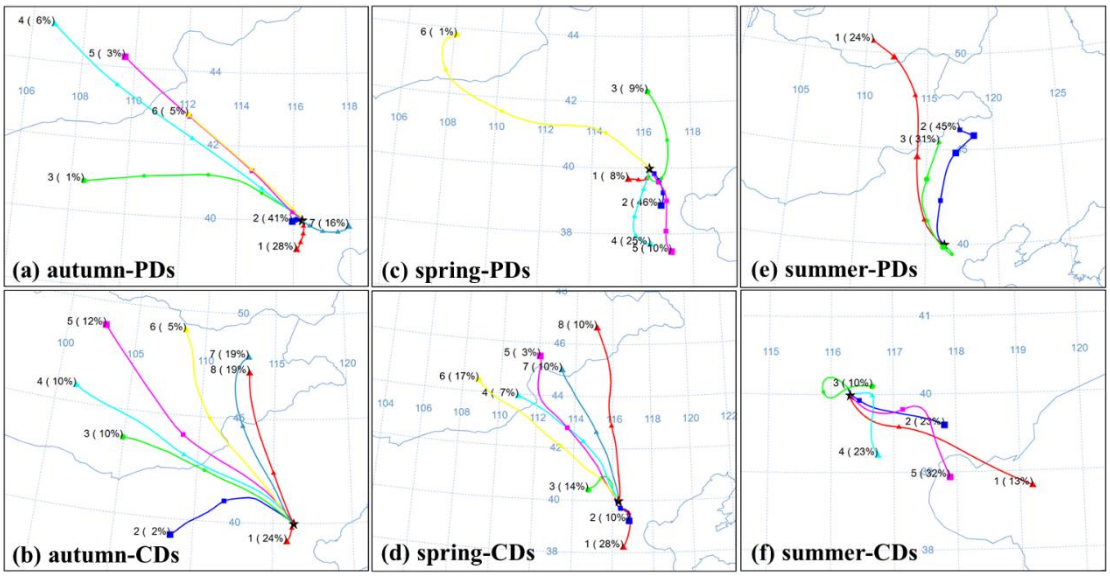

Figure S5. Clustered HYSPLIT backward trajectories during PDs and CDs across different seasons

Table S1. Specifications and functions of fluidic channels in the system

Channel	Flow Rate (mL/min)	Function
Channel 1	0.80 mL/min	Transport ROS_g test solution to the first premixing chamber
Channel 2	1.00 mL/min	Transport DI water to glass spiral coil
Channel 3	0.15 mL/min	Transport DCFH solution to the first premixing chamber
Channel 4	0.15 mL/min	Transport HRP solution to the first premixing chamber
Channel 5	1.50 mL/min	Discharge waste liquid
Channel 6	0.15 mL/min	Transport DCFH solution to the second premixing chamber
Channel 7	0.15 mL/min	Transport HRP solution to the second premixing chamber
Channel 8	1.50 mL/min	Transport DI water to the rotating wet annular denuder
Channel 9	0.80 mL/min	Transport ROS_p test solution to the second premixing chamber
Channel 10	1.00 mL/min	Transport DI water to the spray growth collection chamber
Channel 11	1.50 mL/min	Discharge waste liquid

Table S2. Seasonal statistics of ROS and associated atmospheric species under clean and polluted conditions.

Parameter	Autumn			Winter			Spring			Summer		
	CDs	PDs	Mean	CDs	PDs	Mean	CDs	PDs	Mean	CDs	PDs	Mean
ROS_g (ppbv)	0.89	1.34	1.03	1.22	/	1.22	2.10	3.02	2.28	1.04	1.29	1.16
ROS_p ($\mu g\ m^{-3}$)	0.16	0.13	0.15	0.23	/	0.23	0.45	0.45	0.45	0.24	0.41	0.33
O_3 (ppbv)	24.70	28.07	26.39	29.5	/	29.5	60.60	104.74	82.67	59.42	101.28	80.35
$j(O^1D)$	1.84E-6	1.81E-6	1.83E-6	1.71E-6	/	1.71E-6	4.52E-6	7.13E-6	5.09E-6	1.03E-5	1.04E-5	1.03E-5
$PM_{2.5}$ ($\mu g\ m^{-3}$)	33.45	94.88	52.86	16.1	/	16.1	24.63	40.17	28.04	23.51	27.49	25.30
NO (ppbv)	19.53	26.07	21.59	14.4	/	14.4	10.15	12.33	10.63	9.10	12.93	10.83
NO_2 (ppbv)	18.98	20.36	19.42	11.3	/	11.3	2.63	5.05	3.16	1.32	2.28	1.75
SO_2 (ppbv)	0.56	0.55	0.56	1.03	/	1.03	0.54	0.45	0.52	0.25	0.28	0.27
HONO (ppbv)	0.97	1.73	1.21	0.34	/	0.34	0.40	0.68	0.46	0.64	0.85	0.74
NH_3 (ppbv)	16.74	24.62	19.23	5.54	/	5.54	17.01	29.22	19.69	27.22	21.73	24.75
HNO_3 (ppbv)	0.43	0.80	0.55	0.13	/	0.13	0.20	0.28	0.22	0.30	0.46	0.37
Isoprene (ppbv)	0.05	0.06	0.05	0.02	/	0.02	0.00	0.00	0.00	1.38	1.51	1.45
Alkenes (ppbv)	0.46	0.62	0.51	0.26	/	0.26	0.41	0.48	0.43	0.22	0.20	0.21
T (K)	281.96	283.84	282.55	271.22	/	271.22	292.41	297.17	293.45	301.73	302.76	302.19
RH	0.67	0.78	0.70	0.4	/	0.44	0.45	0.57	0.47	0.67	0.49	0.59
Wind Speed ($m\ s^{-1}$)	1.68	1.19	1.52	2.21	/	2.21	2.61	2.27	2.53	2.05	1.81	1.94

Table S3. Summary of reported ROS concentrations from previous field observations

Phase	season	Site	Mean	Max	Min	Reference
ROS_g (ppbv)	Autumn	Beijing, China (2024)	1.03	2.32	0.07	This study
		Beijing, China (2015)	0.36	0.42	0.25	(Qin et al., 2024)
		Wangdu, China (2017)	0.17	1.00	0.05	(Ye et al., 2021a)
		Gwangju, Korea (2002)	0.28	0.89	0.02	(Hong et al., 2008)
	Winter	Beijing, China (2024)	1.22	2.46	0.07	This study
		Beijing, China (2016)	0.44	/	/	(Huang et al., 2016)
		Beijing, China (2017)	0.25	0.90	0.25	(Ye et al., 2018)
		Manaus, Brazil (2022)	0.30	1.94	0.07	(Hamryszczak et al., 2023)
	Spring	Beijing, China (2025)	2.32	6.82	0.07	This study
		Beijing, China (2016)	0.25	/	/	(Huang et al., 2016)
		Taian, China (2018)	2.05	5.36	0.05	(Ye et al., 2021b)
		Zion, US (2017)	2.10	8.00	0.50	(Vermeuel et al., 2019)
	Summer	Beijing, China (2025)	1.19	4.09	0.07	This study
		Wangdu, China (2014)	0.51	11.3	0.01	(Wang et al., 2016)
		Seoul, Korea (2002)	0.77	5.19	0.04	(Hong et al., 2008)
		St. Louis, United States (2020)	0.04	0.05	0.02	(Eftekhari et al., 2021)
ROS_p ($\mu g\ m^{-3}$)	Autumn	Beijing, China (2024)	0.15	0.35	0.006	This study
		Beijing, China (2015)	0.33	0.46	0.24	(Qin et al., 2024)
		Milan, Italy (2013)	0.01	0.01	0.003	(Perrone et al., 2016)
		Bern, Switzerland (2014)	0.07	0.10	0.04	(Zhou et al., 2019)
	Winter	Beijing, China (2024)	0.23	0.81	0.03	This study
		Beijing, China (2016)	0.45	/	/	(Huang et al., 2016)
		Shanghai, China (2023)	0.09	/	/	(Liu et al., 2023)
		Milan, Italy (2013)	0.01	0.02	0.01	(Perrone et al., 2016)
	Spring	Beijing, China (2025)	0.39	0.98	0.06	This study
		Beijing, China (2016)	0.19	/	/	(Huang et al., 2016)
		Beijing, China (2012)	0.01	0.01	0.0031	(Liu et al., 2014)
		Austin, United States (2012)	0.05	0.13	0.0024	(Khurshid et al., 2014)
	Summer	Beijing, China (2025)	0.39	2.35	0.006	This study
		Beijing, China (2015)	0.44	/	/	(Qin et al., 2024)
		Rochester, United States (2011)	16.90	/	/	(Wang et al., 2011)
		St. Louis, United States (2020)	0.09	0.14	0.03	(Eftekhari et al., 2021)

Reference

Eftekhari, A., Fortenberry, C. F., Williams, B. J., Walker, M. J., Dang, A., Pfaff, A., Ercal, N., and Morrison, G. C.: Continuous measurement of reactive oxygen species inside and outside of a residential house during summer, Indoor Air, 31, 1199-1216, https://doi.org/10.1111/ina.12789, 2021.

Hamryszczak, Z., Hartmann, A., Dienhart, D., Hafermann, S., Brendel, B., Königstedt, R., Parchatka, U., Lelieveld, J., and Fischer, H.: HYPHOP: a tool for high-altitude, long-range monitoring of hydrogen peroxide and higher organic peroxides in the atmosphere, Atmospheric Measurement Techniques Discussions, 2023, 1-25, https://doi.org/10.5194/amt-16-4741-2023, 2023.

Hong, S. B., Kim, G. S., Kang, C. H., and Lee, J. H.: Measurement of ambient hydroperoxides using an automated HPLC system and various factors which affect variations of their concentrations in Korea, Environmental monitoring and assessment, 147, 23-34, https://doi.org/10.1007/s10661-007-0094-4, 2008.

Huang, W., Zhang, Y., Zhang, Y., Zeng, L., Dong, H., Huo, P., Fang, D., and Schauer, J. J.: Development of an automated sampling-analysis system for simultaneous measurement of reactive oxygen species (ROS) in gas and particle phases: GAC-ROS, Atmospheric environment, 134, 18-26, https://doi.org/10.1016/j.atmosenv.2016.03.038, 2016.

Khurshid, S. S., Siegel, J. A., and Kinney, K. A.: Indoor particulate reactive oxygen species concentrations, Environmental research, 132, 46-53, https://doi.org/10.1016/j.envres.2014.03.026, 2014.

Liu, Q., Zhang, Y., Liu, Y., and Zhang, M.: Characterization of springtime airborne particulate matter-bound reactive oxygen species in Beijing, Environmental Science and Pollution Research, 21, 9325-9333, https://doi.org/10.1007/s11356-014-2843-6, 2014.

Liu, Y., Tang, X., Zhang, Z., Li, L., and Chen, J.: Development and Field Testing of an Online Monitoring System for Atmospheric Particle-Bound Reactive Oxygen Species (ROS), Atmosphere, 14, 924, https://doi.org/10.3390/atmos14060924, 2023.

Perrone, M. G., Zhou, J., Malandrino, M., Sangiorgi, G., Rizzi, C., Ferrero, L., Dommen, J., and Bolzacchini, E.: PM chemical composition and oxidative potential of the soluble fraction of particles at two sites in the urban area of Milan, Northern Italy, Atmospheric Environment, 128, 104-113, https://doi.org/10.1016/j.atmosenv.2015.12.040, 2016.

Qin, Y., Zhang, X., Huang, W., Qin, J., Hu, X., Cao, Y., Zhao, T., Zhang, Y., Tan, J., and Zhang, Z.: Measurement report: Impact of emission control measures on environmental persistent free radicals and reactive oxygen species–A short-term case study in Beijing, Atmospheric Chemistry and Physics, 24, 8737-8750, https://doi.org/10.5194/acp-24-8737-2024, 2024.

Vermeuel, M. P., Novak, G. A., Alwe, H. D., Hughes, D. D., Kaleel, R., Dickens, A. F., Kenski, D., Czarnetzki, A. C., Stone, E. A., and Stanier, C. O.: Sensitivity of ozone production to NO_x and VOC along the Lake Michigan coastline, Journal of Geophysical Research: Atmospheres, 124, 10989-11006, https://doi.org/10.1029/2019JD030842, 2019.

Wang, Y., Hopke, P. K., Sun, L., Chalupa, D. C., and Utell, M. J.: Laboratory and Field Testing of an Automated Atmospheric Particle-Bound Reactive Oxygen Species Sampling-Analysis System, Journal of Toxicology, 2011, 419476, https://doi.org/10.1155/2011/419476, 2011.

Wang, Y., Chen, Z., Wu, Q., Liang, H., Huang, L., Li, H., Lu, K., Wu, Y., Dong, H., and Zeng, L.: Observation of atmospheric peroxides during Wangdu Campaign 2014 at a rural site in the North China Plain, Atmospheric Chemistry and Physics, 16, 10985-11000, https://doi.org/10.5194/acp-16-10985-2016, 2016.

Ye, C., Chen, H., Hoffmann, E. H., Mettke, P., Tilgner, A., He, L., Mutzel, A., Brüggemann, M., Poulain, L., and Schaefer, T.: Particle-phase photoreactions of HULIS and TMIs establish a strong source of H_2O_2

and particulate sulfate in the winter North China Plain, Environmental Science & Technology, 55, 7818-7830, https://doi.org/10.1021/acs.estlett.8b00579, 2021a.

Ye, C., Liu, P., Ma, Z., Xue, C., Zhang, C., Zhang, Y., Liu, J., Liu, C., Sun, X., and Mu, Y.: High H_2O_2 concentrations observed during haze periods during the winter in Beijing: importance of H_2O_2 oxidation in sulfate formation, Environmental Science & Technology Letters, 5, 757-763, https://doi.org/10.1021/acs.estlett.8b00579, 2018.

Ye, C., Xue, C., Zhang, C., Ma, Z., Liu, P., Zhang, Y., Liu, C., Zhao, X., Zhang, W., and He, X.: Atmospheric hydrogen peroxide (H_2O_2) at the foot and summit of Mt. Tai: Variations, sources and sinks, and implications for ozone formation chemistry, Journal of Geophysical Research: Atmospheres, 126, e2020JD033975, https://doi.org/10.1029/2020JD033975, 2021b.

Zhou, J., Elser, M., Huang, R.-J., Krapf, M., Fröhlich, R., Bhattu, D., Stefenelli, G., Zotter, P., Bruns, E. A., and Pieber, S. M.: Predominance of secondary organic aerosol to particle-bound reactive oxygen species activity in fine ambient aerosol, Atmospheric Chemistry and Physics, 19, 14703-14720, https://doi.org/10.5194/acp-19-14703-2019, 2019.